Journal of Colloid and Interface Science 560 (2020) 458–466

Contents lists available at ScienceDirect

Journal of Colloid and Interface Science

journal homepage: www.elsevier.com/locate/jcis

Regular Article

Surface chemistry and spectroscopic studies of the native phenylalanine dehydrogenase Langmuir monolayer at the air/aqueous NaCl interface

Rafael Leonardo Cruz Gomes da Silva [a], Shiv K. Sharma [b], Suraj Paudyal [b], Keenan J. Mintz [b], Luciano Caseli [a,*], Roger M. Leblanc [b,*]

[a] Department of Chemistry, Federal University of São Paulo, Diadema, Sao Paulo, Brazil
[b] Department of Chemistry, University of Miami, 1301 Memorial Drive, Coral Gables, Florida 33146, United States

GRAPHICAL ABSTRACT

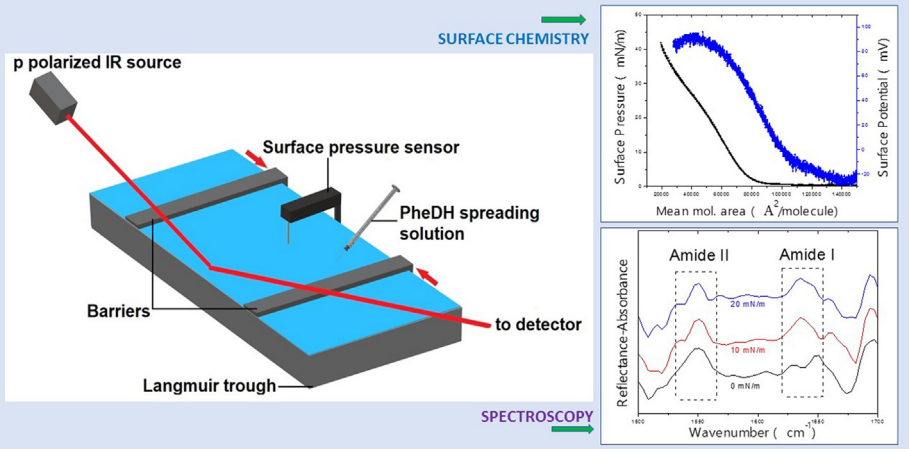

ARTICLE INFO

Article history:
Received 24 September 2019
Revised 18 October 2019
Accepted 21 October 2019
Available online 24 October 2019

Keywords:
Phenylalanine dehydrogenase
Langmuir monolayer
Surface chemistry
Reflectance-absorbance infrared spectroscopy
Langmuir-Blodgett film

ABSTRACT

This study investigates the main aspects of the surface behavior of the native phenylalanine dehydrogenase (PheDH) enzyme at the air/aqueous interface employing a saline subphase to induce the enzyme surface activity. Surface chemistry experiments were performed in order to determine the surface packing and stability of the formed layer, while spectroscopic experiments provided information regarding its secondary structure conformation. It was found that the PheDH enzyme forms a fluid film, which is quite homogeneous throughout its entire compression, being stable for long periods of time with no significant evidence of aggregates or irreversible domains during interfacial compression/decompression processes. The main secondary structures of the interfacial PheDH film were accessed via *in situ* reflectance-absorbance infrared spectroscopy, indicating a majority presence of α-helices, which were maintained after the film transfer to solid muscovite supports. The immobilized films presented a homogeneous and regular deposition, with controlled roughness and a mean thickness in the range of 8–10 nm.

© 2019 Elsevier Inc. All rights reserved.

* Corresponding authors.
E-mail addresses: lcaseli@unifesp.br (L. Caseli), rml@miami.edu (R.M. Leblanc).

https://doi.org/10.1016/j.jcis.2019.10.086
0021-9797/© 2019 Elsevier Inc. All rights reserved.

1. Introduction

Enzymes are biomolecules responsible for the metabolism of all living organisms. They increase the rate of biochemical reactions by lowering the activation energy in the conversion of reactants to products so that most biological processes happen at a perceptible rate. Particularly, the phenylalanine dehydrogenase enzyme (EC 1.4.1.20; PheDH) belongs to the oxidoreductase class of enzymes and is responsible for the reversible oxidative deamination of L-phenylalanine (L-phe) to phenylpyruvate in the presence of nicotinamide adenine dinucleotide in its oxidized form (NAD^+) as an electron acceptor [1]. There are different types of PheDH within a long range of structures and molecular weights. PheDHs from *Sporosarcina* [1–2], *Bacillus* [2] and *Microbacterium* [3] are octameric enzymes, while PheDHs from *Rhodococcus sp* [4], *R. Maris* [5] and *Nocardia* [6] are tetrameric, dimeric and monomeric, respectively. The molecular weight of PheDH ranges from 42,000 (the monomeric *Nocardia* enzyme) to 331,480 (the octameric *B. Sphaericus* enzyme) and the optimum pH of the reversible oxidative deamination of L-phe ranges from 10.4 to 11.3 [2].

In addition to different structures and molecular weights, the class of the PheDH enzymes also presents differences in terms of substrate specificity and kinetic properties. While the PheDH enzymes from *B. badius* and *S. ureae* show a narrow substrate specificity for the L-phe oxidative deamination, the class of PheDHs from *B. Sphaericus* presents good affinity towards the oxidation of L-tyrosine and its keto analog. Moreover, PheDHs from other microorganisms may even present higher specificity for the reductive amination of phenylpyruvate [7]. For this reason enzymes from *B. badius, S. ureae* and its mutants expressed by *E. coli* are extensively studied in the micro-determination of L-phe [8–16]. This is an important component related to phenylketonuria disease (PKU), a genetic disorder characterized by L-phe conversion to phenylpyruvic acid, which is an important neurotoxic component related to impaired neurophysiological functioning and reduced cognitive development in infants [17].

The interaction of biomolecules with different types of interfaces is a subject with its own importance inside the area of surface chemistry, especially when it comes to the development of organo electronic devices [18–22]. The research field of enzyme films has grown considerably in the past few years due to the catalytical power of this class of biocompounds, which allows the buildup of smart surfaces capable of tracing chemical compounds at very low limits of detection and quantification [20,23,24]. However, the production of enzymatic molecular structures is not trivial and requires detailed knowledge of the structure, composition and stability of the system under study.

In this context, the Langmuir technique may be considered an effective way for the production of monomolecular films at the air/aqueous interface with high control over its structure and composition [25]. Important information about the surface packing, phase transitions, dipole orientation and stability of molecular layers can be obtained from classic experiments by monitoring variations in the surface pressure and surface potential isothermally. Also, spectroscopic techniques specially designed for adsorbed molecular films can also be employed in order to obtain detailed information about the film structure [26,27]. The infrared reflection–absorption spectroscopy (IRRAS), for instance, might be highlighted as one of the most widely used techniques to access the orientation of adsorbed surface molecules by using a p-polarized infrared beam sensible to the orientation of dipole moments at the interface [28]. Other important spectroscopic techniques also include the use of *in situ* UV–vis absorbance and fluorescence emission in the investigation of film homogeneity and circular dichroism (CD) spectra in the studies of secondary structures of Langmuir monolayers transferred to solid supports.

To the best of our knowledge the PheDH enzyme has never had its surface activity reported at the air-aqueous interface. Therefore, classical surface pressure experiments were employed in order to access PheDH surface packing and compressibility. Investigations over the stability and surface dipole orientation of PheDH molecules were accessed via compression-decompression cycles, stability curves, surface pressure and surface potential experiments. Finally, *in situ* spectroscopic techniques (IRRAS, UV–vis and Fluorescence) provided important information about the PheDH floating monolayers secondary structure and homogeneity. The structure and morphology of the enzyme layers transferred to solid supports were accompanied *via* circular dichroism and atomic force microscopy.

2. Materials and methods

2.1. Chemicals

Phenylalanine dehydrogenase from Spo*rosarcina* sp. was obtained from Sigma-Aldrich in a high purity lyophilized powder form ($\geq$ 6 units mg^{-1}) and dissolved in ultrapure water with a resistivity of 18.2 MΩ cm, surface tension of 72.1 mN m^{-1} and a pH of 6.0 ± 0.5 at 20.0± 1 °C. The NaCl subphase was prepared with a molecular biology grade NaCl from MP Biomedicals, LLC.

2.2. Equipment

Every experiment was conducted in a clean room (class 1000) in which the temperature (20.0 ± 1 °C) and the humidity (50% ± 1) were maintained constant. Surface chemistry data (π-A and ΔV isotherms, compression-decompression cycles, adsorption and stability curves) were obtained in a Kibron μ-trough (Kibron Inc., Helsinki, Finland) with a 124.5 cm^2 surface area. In situ spectroscopic experiments (UV–vis and Fluorescence) were performed in a KSV mini-trough (KSV Instruments Ltd., Helsinki, Finland) with a 225 cm^2 surface area.

2.3. Langmuir monolayer preparations

PheDH enzyme solutions were prepared in pure water (pH 6.0 ± 0.5) at a concentration of 0.42 μM (0.13 mg mL^{-1}) and spread uniformly at the interface of a 0.1 M sodium chloride subphase with a 100 μL syringe (Hamilton Co., Reno, Nevada). The enzyme volume of 30 μL was spread for the surface chemistry and spectroscopic experiments, with an equilibrium time of 10–20 min before every measurement and a compression rate of 7000 A^2 - $molecule^{-1}$ min^{-1}. The experiments were repeated to assure reliable reproducibility.

2.4. UV–vis spectroscopy

The *in-situ* UV–vis absorption spectra of the PheDH monolayers were taken with the help of an 8452A HP spectrometer fixed on a rail close to the KSV trough (KSV Instruments Ltd., Helsinki, Finland).

2.5. Fluorescence spectroscopy

The *in-situ* fluorescence spectra of the PheDH monolayers were measured with the help of an optical fiber detector on the top of the KSV trough, which was coupled to a Spex Fluorolog fluorespectrometer (Horiba, Jovin Yvon, Edison, NJ). The optical fiber used in

the experiments has an area of 0.25 cm^2 and rested approximately 1 mm above the surface of the subphase.

2.6. Infrared spectroscopy

A Bruker Equinox 55 FTIR (Billerica, MA) equipped with the XA-511 accessory for the air-water interface was used to obtain the infrared spectra of the PheDH monolayer. The measurements were carried out using a p-polarized light and a mercury-cadmium-telluride (MCT) liquid-nitrogen-cooled detector. Each spectrum was acquired by the coaddition of 2048 scans at a resolution of 8 cm^{-1} and a beam incidence angle of 60°.

2.7. Langmuir-Blodgett films preparation

The transfer of preformed PheDH monolayers to solid supports (quartz slides and muscovite) was carried out by raising the slides up from the NaCl aqueous subphase to the air phase at a 2 mm min^{-1}.

2.8. Circular dichroism

Circular Dichroism spectra were obtained for the PheDH enzyme dissolved in water and for the Langmuir-Blodgett film of a single layer transferred to the surface of a quartz solid support with a JASCO J-810 spectropolarimeter.

2.9. AFM images

Images for the PheDH Langmuir-Blodgett films were obtained in tapping mode using an Agilent Technologies microscope model 5420 using a tip with a thickness of 5.0 μm, length of 225 μm and force constant 20 N m^{-1}. The parameters employed were a resonance frequency of 110 kHz, a scan rate of 1.0 Hz and a scan area of 10 × 10 μm. The transferred PheDH films were rinsed with deionized water and dried before AFM measurements.

3. Results and discussion

3.1. Surface pressure and surface potential-area isotherms

The interfacial behavior of PheDH Langmuir monolayer was studied spreading 30 μL of a 0.42 μM PheDH solution on the subphase of a 0.1 M NaCl solution. Different concentrations of NaCl (0.05, 0.1, 0.2, 0.3 and 0.5 M) were tested for the aqueous subphase in order to check the *salting out* effect on the number of PheDH molecules adsorbed at the air-aqueous interface. As presented in Fig. 1, the difference in the lift-off area from the 0.05 M to the 0.1 M NaCl solution (83,407 and 89,229 A^2 $molecule^{-1}$, respectively) indicates an increasing in the number of molecules at the air-aqueous interface when the salt concentration is doubled. No substantial increase in the lift-off area was observed for the 0.2 and 0.3 M isotherms, which indicates no substantial changes in PheDH adsorption. Concentrations of 0.5 M (or superior) produced films with an increased lift-off area, however, the compression profile of the film (and its compressibility) remained the same. On the basis of salt effect on the surface-pressure area isotherms, an ionic concentration of 0.1 M NaCl in the subphase was selected for all further surface chemistry experiments.

It is also worth mentioning that the PheDH enzyme presented surface activity when deionized water was used as subphase, but the obtained surface pressure-area isotherms were not reproducible, indicating instability due to dynamic processes of desorption-adsorption or other molecular rearrangements at the air-water interface.

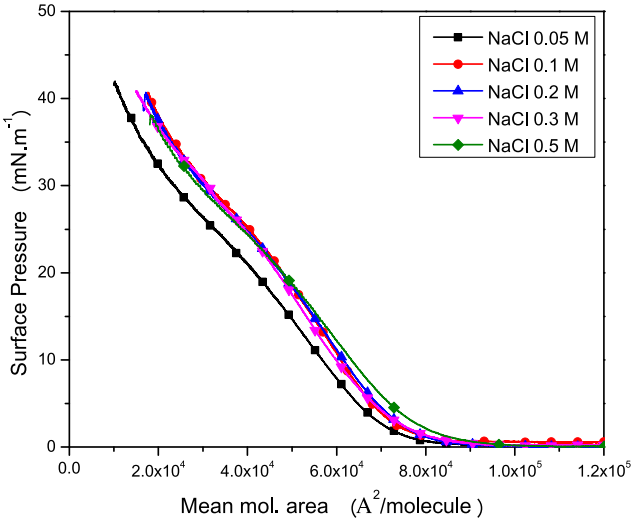

Fig. 1. Surface pressure-Area isotherms for different NaCl concentrations in the subphase (pH 6.0 ± 0.5; Temperature 20.0 ± 1.

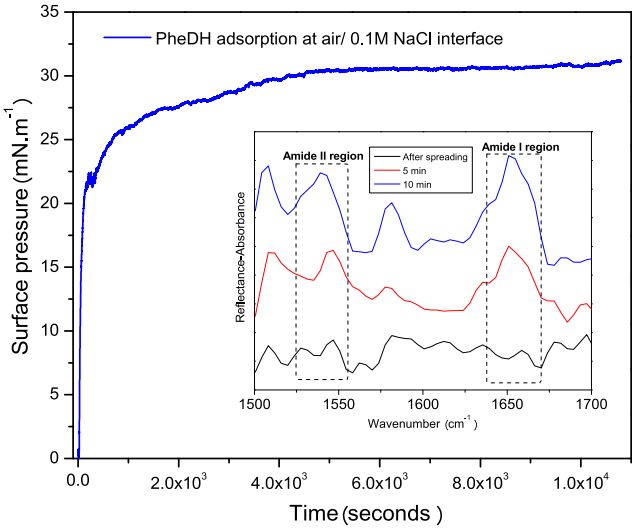

Fig. 2. PheDH adsorption kinetics at the air-NaCl subphase (0.1 M; pH 6.0 ±0.5) for a 3000 mm^2 surface area. Inset presents the p-polarized Reflectance-Absorbance Infrared spectra in different times for the PheDH monolayer at 0 mN m^{-1}.

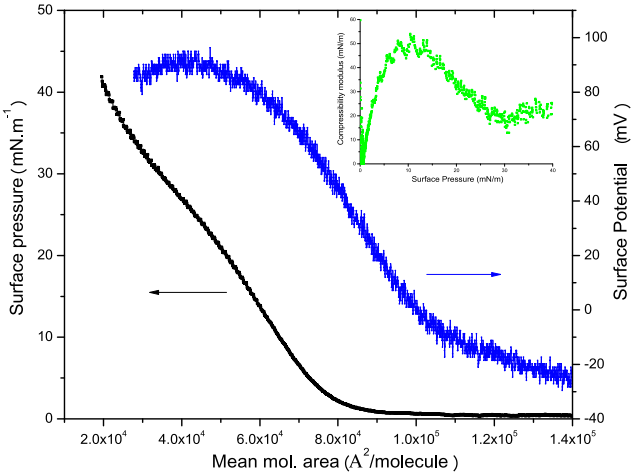

Fig. 3. Surface pressure and surface potential isotherms for the PheDH enzyme (0.13 mg mL^{-1}) the air- NaCl subphase (0.1 M; pH 6 ± 0.5). Inset shows the compressibility modulus for the enzyme throughout its compression.

According to Fig. 2, most of the enzyme adsorption at the interface occurred in the first 1200 s, with a maximum surface pressure of 30 mN m^{-1}. The inset graph shows the enzyme adsorption via reflectance-absorbance infrared spectroscopy (IRRAS) by monitoring the arising of Amide I and Amide II bands (1650 and 1540 cm^{-1}, respectively), attributed respectively to the C═O stretching vibration and to the N—H bending coupled with C—N stretching vibrations of the peptide-backbone [24]. Following the adsorption profile - further surface chemistry experiments were performed within a 20 min lag time after spreading for PheDH adsorption equilibrium to be attained.

Table 1
In plane elasticity values for different bidimensional phases.

C_s^{-1} values (mN m^{-1})	Monolayer Phase
0–12.5	Gaseous
12.5–50	Liquid-expanded
50–100	Liquid
100–250	Liquid-condensed
> 250	Condensed (solid)
0 or < 1	Collapse

The surface pressure and surface potential isotherms obtained for the PheDH monolayer are shown in Fig. 3. From the surface pressure-Area profile (black curve), one can say that for surface areas superior than 90,000 A^2 $molecule^{-1}$, the monolayer is in its gaseous phase and the interaction between neighbor PheDH molecules might be considered negligible. As the area available per molecule is decreased (by the compression of the surface film) a progressive increase in the surface pressure could be observed, meaning that PheDH molecules start to interact and new bidimensional phases can be accessed by the surface film. The system reaches surface pressures as high as 40 mN m^{-1} with a minimum cross-sectional area of 86,500 ± 1402 A^2 $molecule^{-1}$.

The inset graph in Fig. 3 shows the compressibility modulus ($C_s^{-1} = -A(\frac{\partial \pi}{\partial A})_T$) of the PheDH monolayer obtained from its surface pressure-area (π-A) isotherm along its compression. The compressibility modulus – also called in-plane elasticity, or bidimensional elasticity – is a rheological parameter related to the resistance of certain material to be compressed in the static *regime*, and it is directly proportional to the compaction of a Langmuir monolayer. From the value of C_s^{-1}, the phase transitions encountered for a given state of the monolayer [29] can be identified, as shown in Table 1.

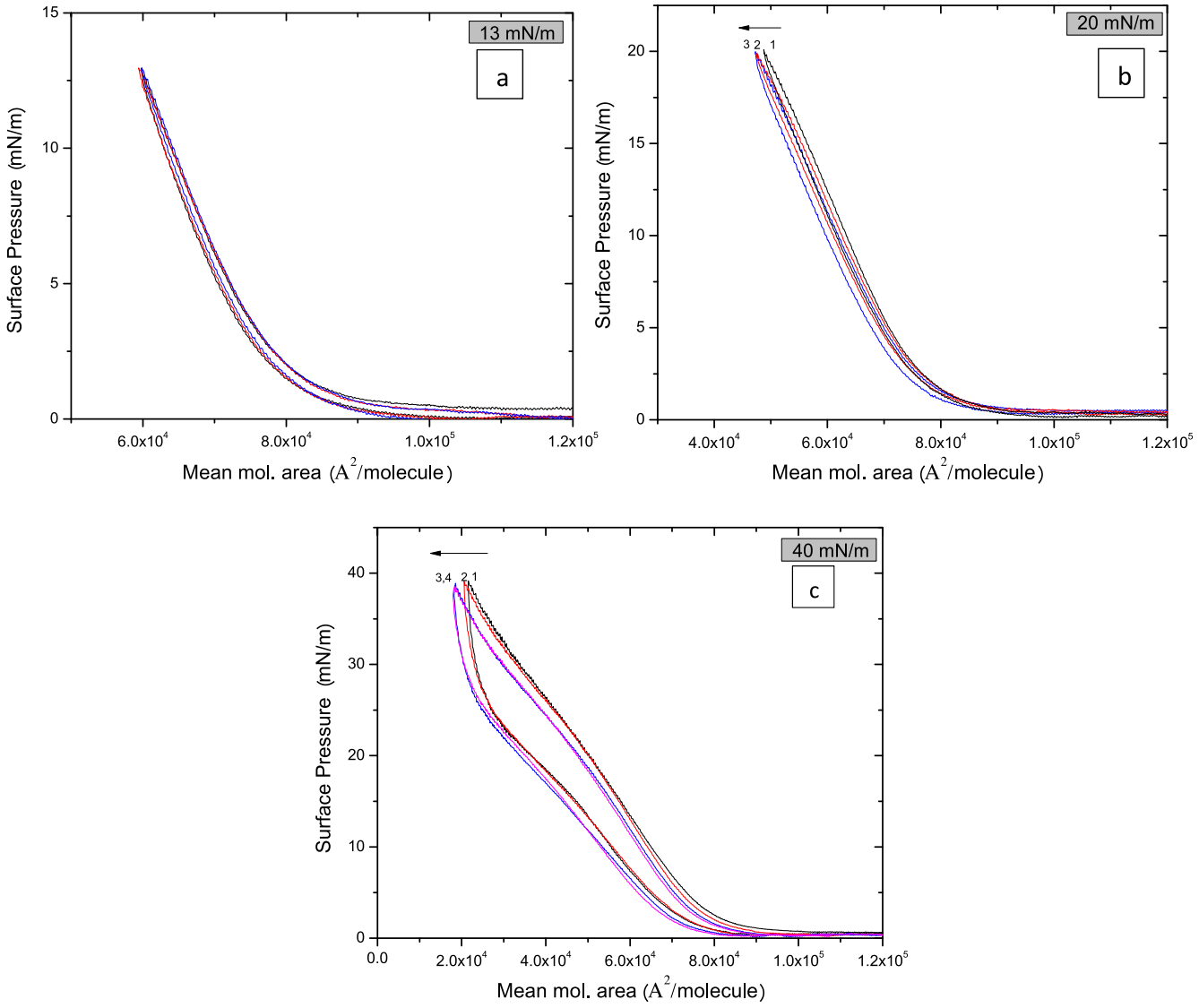

Fig. 4. Compression-decompression cycles for PheDH monolayer at different surface pressures: (a) 13 mN m^{-1}; (b) 20 mN m^{-1} and (c) 40 mN m^{-1} (pH 6.0 ± 0.5; Temperature 20.0 ± 1).

Once the observed C_s^{-1} values for the surface film were never higher than 50 mN m^{-1} one can say that, right after its gaseous phase, the PheDH monolayer reaches its liquid-expanded phase, which lasts throughout the entire compress process. Low C_s^{-1} values are generally associated to low surface compaction and low rigidity, meaning that the PheDH enzyme forms a fluid interfacial film with low viscoelasticity.

Changes in the dipole moments of the PheDH monolayer were accessed simultaneously with the surface pressure measurement using the surface potential-area technique (blue curve Fig. 3). As observed, the initial surface potential measured at the air/0.1 M NaCl interface is negative (−24 mV) and is related to the presence of the Stern layer [30,31] promptly formed by the adsorption of Na^+ ions from the bulk to the slightly negative charged PheDH film.

As the film is compressed and new bidimensional phases become available the dipole moments associated to the PheDH molecules start to reorient at the interface, overcoming the negative contribution of the Stern layer and leading to an overall increase in the surface potential. The PheDH surface film reaches a maximum surface potential of 88 mV when the film reaches its higher compressibility and the dipole moments are close packed aligned at the interface.

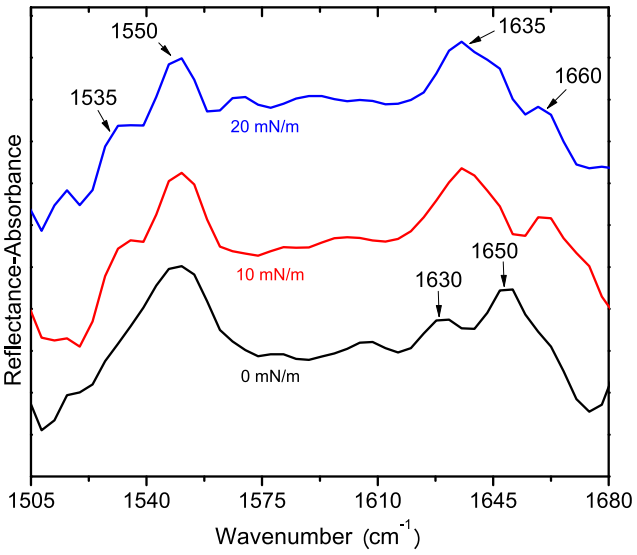

Fig. 6. P-polarized IRRAS spectra for the PheDH monolayer at the surface pressures of 0 mN m^{-1} (black curve), 10 mN m^{-1} (red curce) and 20 mN m^{-1} (blue curve) at pH 6.0 ± 0.5; Temperature 20.0 ± 1. (For interpretation of the references to colour in this figure legend, the reader is referred to the web version of this article.)

3.2. Compression-decompression cycles and stability

Important information about the reversibility and stability of a Langmuir monolayer can be accessed via compression and decompression experiments. If the compression profile observed for a certain monolayer is in close coincidence with the one observed during the decompression, it is said that the monolayer has a good

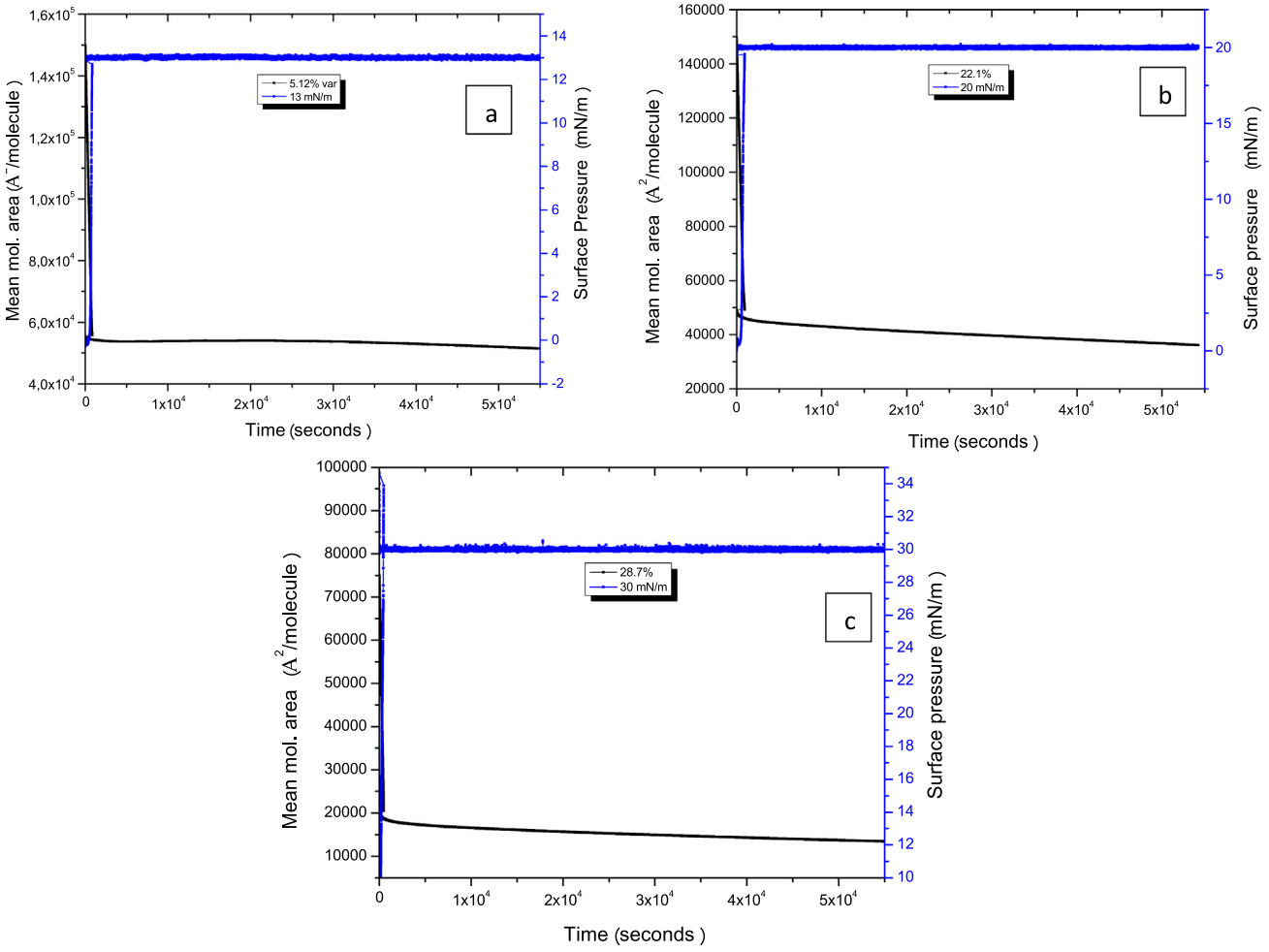

Fig. 5. Stability measurements of the PheDH Langmuir Monolayer at the surface-Pressures of (a) 10 mN m^{-1}; (b) 20 mN m^{-1} and (c) 30 mN m^{-1} in 0, 1 M NaCl subphase (pH 6.0 ± 0.5; Temperature 20.0 ± 1).

reversibility with little material loss to the subphase or formation of kinetic irreversible domains. Three compression-decompression cycles were examined for the stability of the PheDH monolayer at the surface pressures of 13, 20 and 40 mN m^{-1}, as presented in Fig. 4a–c, respectively. For the compression-decompression cycle performed at a low surface pressure (Fig. 4a) it is noted that the PheDH monolayer presents a good reversibility from cycle to cycle with a minimal loss of enzyme molecules to the subphase. The loss of material to the subphase was shortly higher for the intermediary pressure of 20 mN m^{-1}. When the cycles are performed at higher surface pressures the hysteresis increases, which means that the material loss to the subphase becomes apparent.

The stability of PheDH monolayer was also accessed monitoring its mean molecular area variation over a certain period of time for different surface pressures, as presented in Fig. 5. Over 15 h, the approximate mean molecular area change was about 5.12% for the 10 mN m^{-1} monolayer, 22.1% for the 20 mN m^{-1} and 28.7% for the 30 mN m^{-1} indicating a decrease in film stability with the increase in pressure which might be mostly related to dissolution of PheDH molecules into the subphase or conformational changes.

3.3. Infrared reflectance-absorbance spectroscopy

Since its development in the mid-1980's [26,32] the infrared reflectance-absorbance spectroscopy (IRRAS) has been widely used in the study of the conformation and orientation of lipids and biomolecules at the air-aqueous interface [33–35]. In this technique, a p-polarized infrared beam (perpendicular to the interface) impinges onto the surface at a well-defined and controlled angle of incidence interacting with oriented dipoles present on the water surface. The reflected light is detected at an angle equal to the angle of incidence and converted to a reflection-absorption signal (RA). The RA signal is defined as $-\log_{10}(R/R_0)$ where R is the reflectivity of the surface covered by an interfacial layer and R_0 is the reflectivity of the pure aqueous subphase.

The plot of RA *versus* wavenumber is called IRRAS spectra and contains important information about the conformation and structure of adsorbed layers. Conformational changes and the secondary structure of adsorbed biomolecules, like proteins and enzymes, can be accessed by the analysis of the amide bands (Amides I and II). Fig. 6 shows the IRRAS spectra for the PheDH monolayer at a 60-degree angle of incidence. Generally, α-helix structures exhibit amide I (C═O stretching of the peptide bond) and Amide II (N—H bending and C—N stretching of the peptide bond) absorptions in the range of 1650 to 1660 cm^{-1} and 1540 to 1550 cm^{-1}, respectively while β-sheet structures exhibit similar absorption bands at the regions of 1620 to 1630 cm^{-1} and 1520 to 1535 cm^{-1} [36–37].

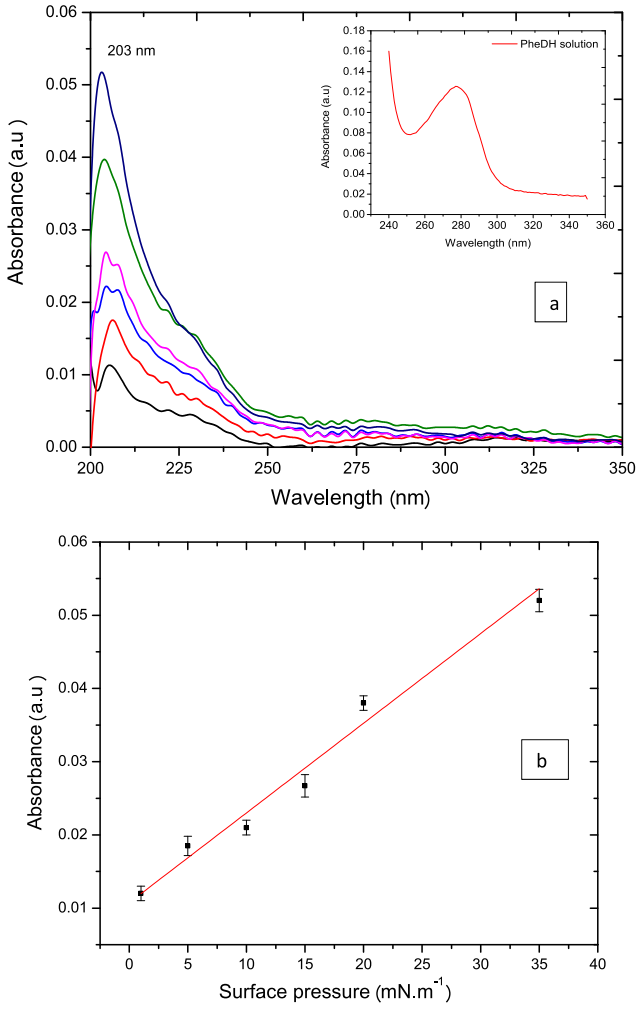

Fig. 7. *In* situ UV–vis absorption spectra for the PheDH monolayer (a). Absorbance signal *versus* Surface Pressure plot (b) for the PheDH monolayer between 0 and 35 mN m^{-1} (pH 6.0 ± 0.5; Temperature 20.0 ± 1). The inset in Fig. 7a shows the UV–vis spectra for a 0.13 mg mL^{-1} PheDH solution.

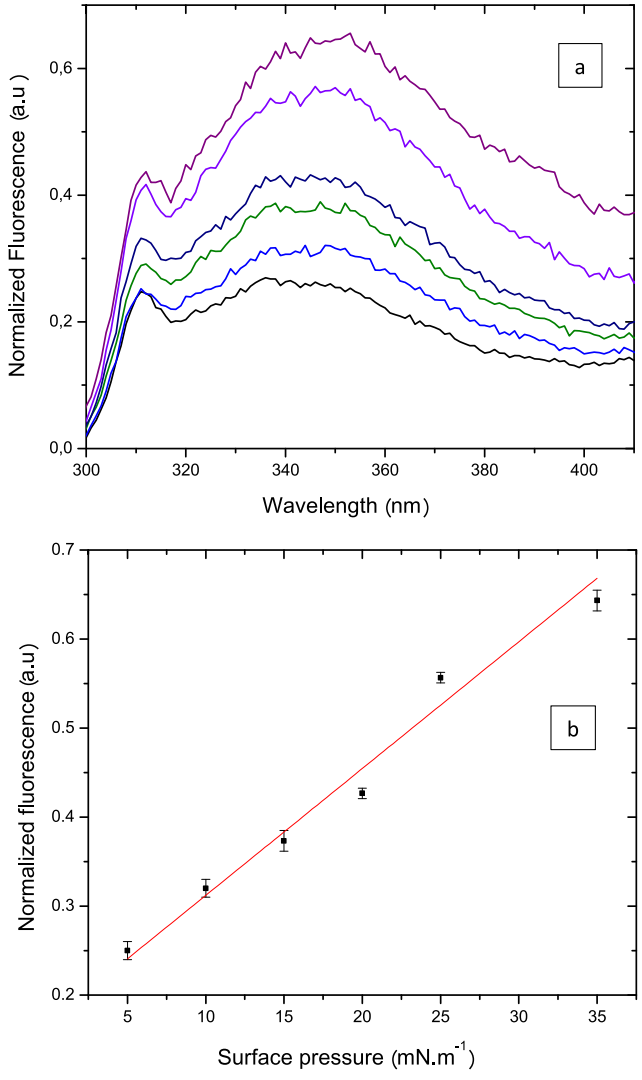

Fig. 8. *In*-situ Fluorescence spectra for the PheDH monolayer (a). Normalized emission signal *versus* Surface Pressure plot (b) for the PheDH monolayer between 5 and 35 mN m^{-1} (pH 6.0 ± 0.5; Temperature 20.0 ± 1).

At the surface pressure of 0 mN m^{-1} (black curve Fig. 6) three main absorption bands can be highlighted: one for the Amide II at 1550 cm^{-1} and two for the Amide I at 1630 and 1650 cm^{-1}. The broad (and more intense) bands assigned at 1550 and 1650 cm^{-1} indicate the majority of α-helix structures for the enzyme in its gaseous phase with a discrete presence of β-turns assigned for the small intensity band at 1630 cm^{-1}.

As the enzyme is compressed towards its liquid-expanded phase, conformational changes may take place leading to differences in the structure of the interfacial PheDH. The spectra for the surface pressures of 10 and 20 mN m^{-1} (red and blue curves, respectively) presented close coincidence for the same set of absorption bands. The 1550 cm^{-1} band related to the α-helix structure (before observed in the gaseous phase) is still present in the liquid-expanded phases, indicating the maintenance of these structures in the monomolecular film. The main structural difference observed for the liquid-expanded PheDH film is highlighted as a broad band at 1635 cm^{-1} which might indicate the presence of unordered structures (random coil structure) exposed to the interface. The shoulder bands highlighted in 1535 and 1660 cm^{-1} are related to β-sheet and α-helix structures, respectively.

It has to be noted that the IRRAS spectra has been taken at surface pressures in which the PheDH monolayer shows an excellent stability (see Fig. 5) during the time of the experiments.

3.4. UV–vis absorption spectroscopy

Important information about the homogeneity of the PheDH monolayer was accessed by UV–vis spectroscopy, as shown in Fig. 7. As the monolayer was compressed and the surface pressure increased, the absorbance for the peak observed at 203 nm increased gradually in a linear fashion. The absorbance peak at 203 nm is related to the n – π* transition for peptide bonds, and the linear increasing with surface pressure is a strong evidence that the monolayer of the PheDH enzyme presents a good homogeneity at the air-subphase interface. The inset graph on Fig. 7a shows the absorbance spectra obtained for a 0.13 mg mL^{-1} solution of PheDH in water. The band observed at 280 nm is related to the tryptophan group present in the 375th position of the primary structure of the PheDH [38]. The absence of the 280 nm band for the PheDH monolayer can be explained by the fact that the amount of tryptophan residue per unit area was too low to be detected.

3.5. Fluorescence spectroscopy

Although no absorbance band for tryptophan residues could be measured using UV–vis spectroscopy (Fig. 7), the *in-situ* fluorescence of the interfacial film presented emission bands for the amino acid at 350 nm when excited at 280 nm, according to Fig. 8. Just like observed for the UV–vis absorption, the fluorescence emission for the PheDH monolayer also increased in a linear fashion with surface pressure (Fig. 8b). This indicates a homogeneous increasing in the surface concentration of tryptophan groups upon compression. Despite the low number of tryptophan residues presented by the film, the high fluorescence quantum yield of the amino acid seemed to play an important role in its interfacial detection.

3.6. Circular dichroism

The far ultraviolet region of the circular dichroism spectra (ranging from 250 to 190 nm) is normally used to analyze the conformation of proteins, providing access to main secondary structures, i.e., α-helix, β-sheet and random coil [39–40]. According to the black and red curves on Fig. 9, two main bands could be attributed to the PheDH enzyme in solution which are related to

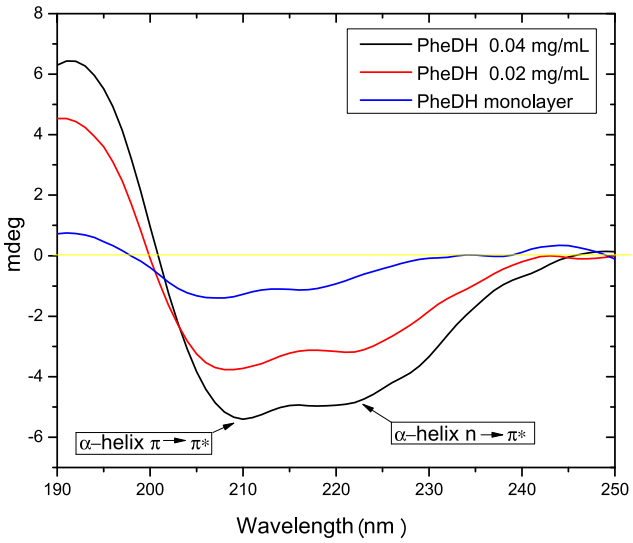

Fig. 9. Circular dichroism spectra in the far UV region for transferred PheDH monolayer at 35 mN m^{-1} (blue curve) and for the enzyme dissolved in deionized water at two different concentrations (black and red curves). (For interpretation of the references to colour in this figure legend, the reader is referred to the web version of this article.)

the π – π* and n – π* transitions for the α-helix structures of the enzyme. Since it is not possible to directly measure the circular dichroism spectra at the air/subphase interface, a singular layer of the interfacial PheDH film was transferred to a solid quartz support via Langmuir-Blodgett (LB) technique.

The LB technique consists in the transfer of an interfacial Langmuir film at a given surface pressure via immersion or withdrawal of a solid support into or from the aqueous subphase. Repeated passages of the solid support can result in the deposition of multilayered structures which gives the LB technique a high control of the architecture over the film immobilization process [41]. Film depositions can be quantified by the calculation of the transfer ratio (TR) which is defined as the ratio between the decrease in the monolayer area during a deposition stroke and the area of the solid support. An ideal deposition has a TR that is equal to 1, meaning that the entire area along the solid support was covered by the Langmuir film. Table 2 presents the results for different values of TR of the PheDH monolayer in different stages of its compaction at the interface. It seems that higher values of surface pressure give TR values close to the unity, indicating a better uniformity.

The blue curve for the circular dichroism spectra on Fig. 8 was obtained for the PheDH monolayer transferred at a surface pressure of 35 mN m^{-1} (highest TR value). As observed the same bands present in the PheDH solutions of 0.02 and 0.04 mg mL^{-1} are present in the LB film spectra indicating that the enzyme is transferred to the solid support without significant changes in its secondary structure, with a predominance of α-helix structures.

The small shift in wavelength for the solution spectra and the one obtained for the transferred film might be related to the scattering of light due to the refractive index of the slide medium.

Table 2
Calculated transfer ratios for PheDH monolayers transferred at different surface pressures.

Transfer Ratio (TR)	Surface-Pressure of transference (mN m^{-1})
0.52	15
0.68	25
0.89	35

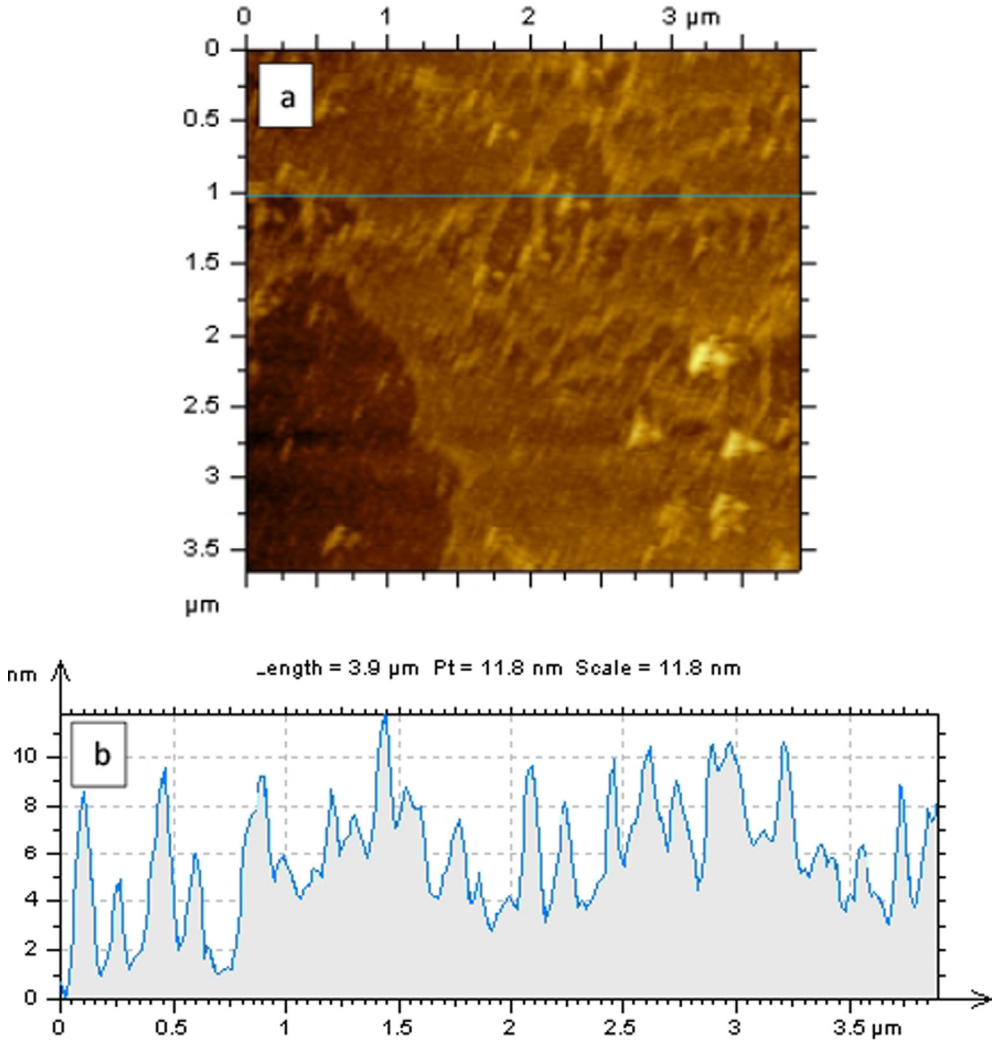

Fig. 10. AFM image of the PheDH layer transferred to a muscovite mica substrate (a) and the extracted height profile (b). The solid support was rinsed and dried several times to remove crystalized NaCl particles.

3.7. AFM images

Atomic force microscopy is a versatile technique to determine the structure and morphology of films adsorbed onto solid supports, especially for compounds with biological relevance such as lipids, proteins, enzymes, *etc* [42]. Since muscovite mica presents a flat surface it produces a smooth surface for AFM imaging which allows the identification of deposited molecules by contrast. Due to the subphase content of sodium chloride, the muscovite supports were rinsed with water and dried, after the enzyme deposition, in order to assure that salt crystals do not interfere in the measurements. Fig. 10a presents the image for the adsorbed layer of PheDH at 35 mN m^{-1} to a muscovite solid support, employing the tapping mode. As one can see, the brighter regions of the image indicate the presence of the enzyme with a quite homogeneous and regular deposition. The lower left corner appears to be the edge of the layer which allows some comparison of height. According to Fig. 10b the PheDH film appears to have a mean thickness in the range of 8–10 nm.

4. Conclusions

Significant aspects about the formation of PheDH monolayers at the air/aqueous NaCl subphase and its transferred films to solid supports were reported in the present work. It was found that (i) the *salting out* effect exerts a major role in the production of stable and reproducible Langmuir monolayers of the enzyme PheDH; (ii) Tensiometric data showed that PheDH adsorbed molecules form a fluid interfacial film with a low surface density of 86,500 A^2-molecule^{-1}; (iii) PheDH monolayer presented a good homogeneity throughout its compression as confirmed by the linear increase in the UV–vis absorption of peptide bonds and in the fluorescence emission of tryptophan residues; (iv) The trends observed in the compression-decompression cycles and stability studies indicated that the interfacial layer presents a decrease in reversibility and stability as it is compressed towards high surface pressures; (v) IRRAS data indicated a predominance of α-helix structures in the floating monolayer along its compression, which was also observed for the immobilized layer, indicating maintenance of the enzyme secondary structures upon its transfer; (vi) AFM images showed that the immobilized film presents a homogeneous and regular deposition, with controlled roughness and a mean thickness in the range of 8–10 nm. In general, we believe that the present work may enrich the understanding on the formation and characterization of enzymes forming Langmuir monolayers and Langmuir-Blodgett films. Also, this work may be particularly important in the design of PheDH covered electrodes for the detection of L-phe as nanostructured biosensors.

Acknowledgements

This work was supported by the São Paulo Research Foundation (FAPESP grant number 2019/01797-6) and developed in a partnership between University of Miami (Miami – Florida) and Federal University of São Paulo (Diadema – São Paulo).

References

[1] Y. Asano, A. Nakazawa, Crystallization of phenylalanine dehydrogenase from Sporosarcina ureae, Agri. Biol. Chem. 49 (1985) 3631–3632.
[2] Y. Asano, A. Nakazawa, K. Endo, Novel phenylalanine dehydrogenases from Sporosarcina ureae and Bacillus sphaericus purification and characterization, *J. Biol. Chem.* 262 (1987) 10346–10354.
[3] Y. Asano, M. Tanetani, Thermostable phenylalanine dehydrogenase from a mesophilic Microbacterium sp. strain DM 86–1, Arch. Microbiol. 169 (1998) 220–224.
[4] Y. Asano, Phenylalanine dehydrogenase. *Encyclopedia of industrial* biotechnology: bioprocess, bioseparation, Cell Technol. (2009) 1–34.
[5] H. Misono, J. Yonezawa, S. Nagata, S. Nagasaki, Purification and characterization of a dimeric phenylalanine dehydrogenase from Rhodococcus maris K-18, J. Bacteriol. 171 (1) (1989) 30–36.
[6] L. De Boer, M. Van Rijssel, G. Euverink, L. Dijkhuizen, Purification, characterization and regulation of a monomeric L-phenylalanine dehydrogenase from the facultative methylotroph Nocardia sp. 239, Arch. Microbiol. 153 (1) (1989) 12–18.
[7] Flickinger, M. C., Encyclopedia of industrial biotechnology: bioprocess, bioseparation, and cell technology, 7 Volume Set. John Wiley & Sons; 2010.
[8] E. Omidinia, S.M. Naghib, A. Boughdachi, P. Khoshkenar, D.K. Mills, Hybridization of silver nanoparticles and reduced graphene nanosheets into a nanocomposite for highly sensitive L-phenylalanine biosensing, Int. J. Electrochem. Sci. 10 (2015) 6833–6843.
[9] S.M. Naghib, M. Rabiee, E. Omidinia, Electrochemical biosensor for L-phenylalanine based on a gold electrode modified with graphene oxide nanosheets and chitosan, Int. J. Electrochem. Sci. 9 (2014) 2341–2353.
[10] S.M. Naghib, M. Rabiee, E. Omidinia, P. Khoshkenara, D. Zeini, Biofunctionalization of dextran-based polymeric film surface through enzyme immobilization for phenylalanine determination, Int. J. Electrochem. Sci. 7 (2012) 120–135.
[11] E. Omidinia, N. Shadjou, M. Hasanzadeh, Electrochemical nanobiosensing of phenylalanine using phenylalanine dehydrogenase incorporated on amino-functionalized mobile crystalline material-41, IEEE Sensors J. 14 (2013) 1081–1088.
[12] D.J. Weiss, M. Dorris, A. Loh, L. Peterson, Dehydrogenase based reagentless biosensor for monitoring phenylketonuria, Biosens. Bioelectron. 22 (2007) 2436–2441.
[13] E. Omidinia, N. Shadjou, M. Hasanzadeh, Immobilization of phenylalanine-dehydrogenase on nano-sized polytaurine: a new platform for application of nano-polymeric materials on enzymatic biosensing technology, Mater. Sci. Eng.: C 42 (2014) 368–373.
[14] R. Villalonga, A. Fujii, H. Shinohara, S. Tachibana, Y. Asano, Covalent immobilization of phenylalanine dehydrogenase on cellulose membrane for biosensor construction, Sens. Actuat. B: Chem. 129 (2008) 195–199.
[15] H. Naruse, Y. Ohashi, A. Tsuji, M. Maeda, K. Nakamura, T. Fujii, A. Yamaguchi, M. Matsumoto, M. Shibata, A method of PKU screening using phenylalanine dehydrogenase and microplate system, Screening 1 (1992) 63–66.
[16] S. Girotti, E. Ferri, S. Ghini, R. Budini, G. Carrea, R. Bovara, S. Piazzi, R. Merighi, A. Roda, Bioluminescent flow sensor for L-phenylalanine determination in serum, Talanta 40 (1993) 425–430.
[17] H. Chandler, J. Cox, K. Healey, A. MacGregor, R. Premier, J. Hurrell, An investigation of the use of urease-antibody conjugates in enzyme immunoassays, J. Immunol. Methods 53 (1982) 187–194.
[18] C.G. Barbosa, L. Caseli, L.O. Péres, Conjugated polymers nanostructured as smart interfaces for controlling the catalytic properties of enzymes, J. Colloid Interface Sci. 476 (2016) 206–213.
[19] R.T. Rodrigues, P.V. Morais, C.S. Nordi, M.J. Schöning, J.R. Siqueira Jr, L. Caseli, Carbon nanotubes and algal polysaccharides to enhance the enzymatic properties of urease in lipid Langmuir-Blodgett films, Langmuir 34 (2018) 3082–3093.
[20] J.M. Rocha, A. Pavinatto, T.M. Nobre, L. Caseli, Acylated carrageenan changes the physicochemical properties of mixed enzyme-lipid ultrathin films and enhances the catalytic properties of sucrose phosphorylase nanostructured as smart surfaces, J. Phys. Chem. B 120 (2016) 5359–5366.
[21] F.A. Scholl, L. Caseli, Langmuir and Langmuir-Blodgett films of lipids and penicillinase: studies on adsorption and enzymatic activity, Colloids Surf. B: Biointerfaces 126 (2015) 232–236.
[22] S.K. Sharma, M. Micic, S. Li, B. Hoar, S. Paudyal, E.M. Zahran, R.M. Leblanc, Conjugation of carbon dots with β-galactosidase enzyme: surface chemistry and use in biosensing, Molecules 24 (2019) 3275–3282.
[23] N.C. Zanon, O.N. Oliveira Jr, L. Caseli, Immbolization of uricase enzyme in Langmuir and Langmuir-Blodgett films of fatty acids: possible use as a uric acid sensor, J. Colloid Interface Sci. 373 (2012) 69–74.
[24] F.T. de Araújo, L. Caseli, Rhodanese incorporated in Langmuir and Langmuir-Blodgett films of dimyristoylphosphatidic acid: physical chemical properties and improvement of the enzyme activity, Colloids Surf. B: Biointerfaces 141 (2016) 59–64.
[25] T.M. Nobre, F.J. Pavinatto, L. Caseli, A. Barros-Timmons, P. Dynarowicz-Łątka, O.N. Oliveira Jr, Interactions of bioactive molecules & nanomaterials with Langmuir monolayers as cell membrane models, Thin Solid Films 593 (2015) 158–188.
[26] R.A. Dluhy, Quantitative external reflection infrared spectroscopic analysis of insoluble monolayers spread at the air-water interface, J. Phys. Chem. 90 (1986) 1373–1379.
[27] C.R. Flach, J.W. Brauner, J.W. Taylor, R.C. Baldwin, R. Mendelsohn, External reflection FTIR of peptide monolayer films in situ at the air/water interface: experimental design, spectra-structure correlations, and effects of hydrogen-deuterium exchange, Biophys. J. 67 (1994) 402–410.
[28] R. Mendelsohn, G. Mao, C.R. Flach, Infrared reflection–absorption spectroscopy: principles and applications to lipid–protein interaction in Langmuir films, B*BA-Biomembranes* 1798 (2010) 788–800.
[29] Stauft, J., JT Davies und EK Rideal. Interfacial Phenomena. Academic Press, New York und London 1961, 66, pp. 453–453.
[30] J. Davies, The distribution of ions under a charged monolayer, and a surface equation of state for charged films, in: Proceedings of the Royal Society of London. Series A. Math. Phys. Sci., 1951, pp. 224–247.
[31] J. Davies, A surface equation of state for charged monolayers, J. Colloid Sci. 11 (1956) 377–390.
[32] S.K. Sharma, E.S. Seven, M. Micic, S. Li, R.M. Leblanc, Surface chemistry and spectroscopic study of a Cholera toxin B Langmuir monolayer, Langmuir 34 (2018) 2557–2564.
[33] G. Thakur, C. Wang, R.M. Leblanc, Surface chemistry and in situ spectroscopy of a lysozyme Langmuir monolayer, Langmuir 24 (2008) 4888–4893.
[34] Z. Xu, J.W. Brauner, C.R. Flach, R. Mendelsohn, Orientation of peptides in aqueous monolayer films. Infrared reflection– absorption spectroscopy studies of a synthetic amphipathic β-sheet, Langmuir 20 (2004) 3730–3733.
[35] S.K. Sharma, S. Li, M. Micic, J. Orbulescu, D. Weissbart, H. Nakahara, O. Shibata, R.M. Leblanc, β-galactosidase Langmuir monolayer at air/x-gal subphase interface, J. Phys. Chem. B 120 (2016) 12279–12286.
[36] W.K. Surewicz, H.H. Mantsch, D. Chapman, Determination of protein secondary structure by Fourier transform infrared spectroscopy: a critical assessment, Biochem. 32 (1993) 389–394.
[37] J.T. Pelton, L.R. McLean, Spectroscopic methods for analysis of protein secondary structure, Anal. Biochem. 277 (2000) 167–176.
[38] Consortium, U., UniProt: a hub for protein information, Nucleic Acids Res. 43 (2014) D204–D212.
[39] N.J. Greenfield, Using circular dichroism spectra to estimate protein secondary structure, Nat. Protoc. 1 (2006) 2876–2880.
[40] S. Li, S. Potana, D.J. Keith, C. Wang, R.M. Leblanc, Isotope-edited FTIR in H 2 O: determination of the conformation of specific residues in a model α-helix peptide by 13 C labeled carbonyls, Chem. Commun. 50 (2014) 3931–3933.
[41] O.N. Oliveira Jr, Langmuir-Blodgett films-properties and possible applications, Braz. J. Phys. 22 (1992) 60–69.
[42] C.M. Yip, Atomic force microscopy of macromolecular interactions, Curr. Opin. Str. Biol. 11 (2001) 567–572.